



Iron Powder Cores for  
Switchmode Power Supply Inductors

by: Jim Cox

**Purpose:** The purpose of this application note is to cover the properties of iron powder as a magnetic core material for inductors in switch-mode power supplies. The different considerations for DC output chokes, differential-mode line filter inductors, power factor correction inductors, and high frequency resonant inductors will be covered.

**Iron Powder as a Core Material:** Iron powder is one of various core materials that are commonly used to produce magnetic components in today's switching power supplies. It is one of the least expensive core materials available. The magnetic properties of iron powder make it a good choice for many inductor applications but it is not a good choice for the main switching transformer.

Iron powder cores are produced from very fine, insulated particles of highly pure iron powder. This prepared powder is compressed under extremely high pressures to produce a solid-looking core. This process creates a magnetic structure with a distributed air-gap. The inherent high saturation flux density of iron combined with the distributed air-gap produces a core material with initial permeabilities of no more than 100 and with high-energy storage capabilities.

The compaction process used to produce iron powder cores is suitable to make a wide variety of configurations. Toroidal cores, E-cores, U-cores, Slugs, and Bus-Bar cores are all available in iron powder. It is possible to provide height variations of existing sizes through press adjustment without the need for separate tooling. It is relatively inexpensive to custom tool a special size or shape. Such tooling will typically cost about \$1000 per inch for the major dimension.

Iron powder can be produced to rather tight tolerances both physically and electrically. It is quite stable with temperature and tolerates the stresses of encapsulation with very little change in properties.

A general material properties table is shown in Figure A on the following page. The material designations (Mix No.) listed in this table will be referred to throughout this paper.



## GENERAL MATERIAL PROPERTIES

Material Mix No.	Reference Permeability ( $\mu_0$ )	Material Density (g/cm <sup>3</sup> )	Relative Cost	Color Code
-2	10	5.0	2.7	Red/Clear
-8	35	6.5	5.0	Yellow/Red
-14	14	5.2	3.6	Black/Red
-18	55	6.6	3.4	Green/Red
-26	75	7.0	1.0	Yellow/White
-30*	22	6.0	1.4	Green/Gray
-34*	33	6.2	1.5	Gray/Blue
-35*	33	6.3	1.4	Yellow/Gray
-38	85	7.1	1.1	Gray/Black
-40	60	6.9	1.0	Green/Yellow
-45	100	7.2	2.6	Black/Black
-52	75	7.0	1.2	Green/Blue

\* The -30 Material was developed as a lower cost, lower loss alternate to the -28 Material. Similarly, the -34 & -35 Materials were developed to replace the -33 Material. The -28 & -33 Materials are not listed in this catalog but are still available.

**Figure A**

The basic magnetic properties are listed along with each material's Color Code and Relative Cost. The relative cost reflects the comparative selling price of a typical one-inch core. Smaller cores will exhibit less difference in price.

Typical Applications for each Material follow:

## MATERIAL APPLICATIONS

Typical Application	-2	-8	-14	-18	-26	-30	-34	-35	-38	-40	-45	-52
Light Dimmer Chokes					X				X	X	X	
60 Hz Differential-mode EMI Line Chokes					X				X	X	X	X
DC Chokes: <50kHz or low Et/N (Buck/Boost)					X	X	X	X	X	X	X	
DC Chokes: ≥50kHz or higher Et/N (Buck/Boost)	X	X	X		X	X	X					X
Power Factor Correction Chokes: <50kHz					X	X	X	X				X
Power Factor Correction Chokes: ≥50kHz	X	X	X	X		X	X	X				
Resonant Inductors: ≥50kHz	X		X									

**General Design Considerations:** The amount of energy an inductor stores (in microjoules) is calculated by multiplying one-half the inductance in microhenries times the current in amperes squared ( $1/2 LI^2$ ). This energy is proportional to the operating flux density squared divided by the effective permeability under those conditions ( $B^2/\mu_{eff}$ ). In the case of high permeability core materials, such as Ferrite's, by introducing an air gap, a significantly lower permeability is realized. This increases the energy storage capabilities of the core by allowing additional energy to be stored in the air gap.



Energy storage inductor designs will be limited by either magnetic saturation or excessive temperature rise resulting from both winding and core losses. In the case of iron powder, due to the fairly low permeability, moderate core loss properties, and very gradual saturation characteristics; designs are almost always limited by temperature rise rather than magnetic saturation.

The gradual DC saturation characteristics of iron powder are shown below in Figure B. It is common for the higher permeability materials like the -26 and -52 to be operated at 50% of their initial permeability. Curve-fit formulas describing these curves are available.

Figure C, at the top of the following page, shows a typical DC energy storage curve for iron powder. This set of curves shows energy storage as a function ampere-turns for the -26 Material where essentially all of the current flowing is DC. This implies that the AC content is of sufficiently low level so as to not generate any noticeable core loss. It can be seen that as more ampere-turns are applied to a core, that more energy storage results.

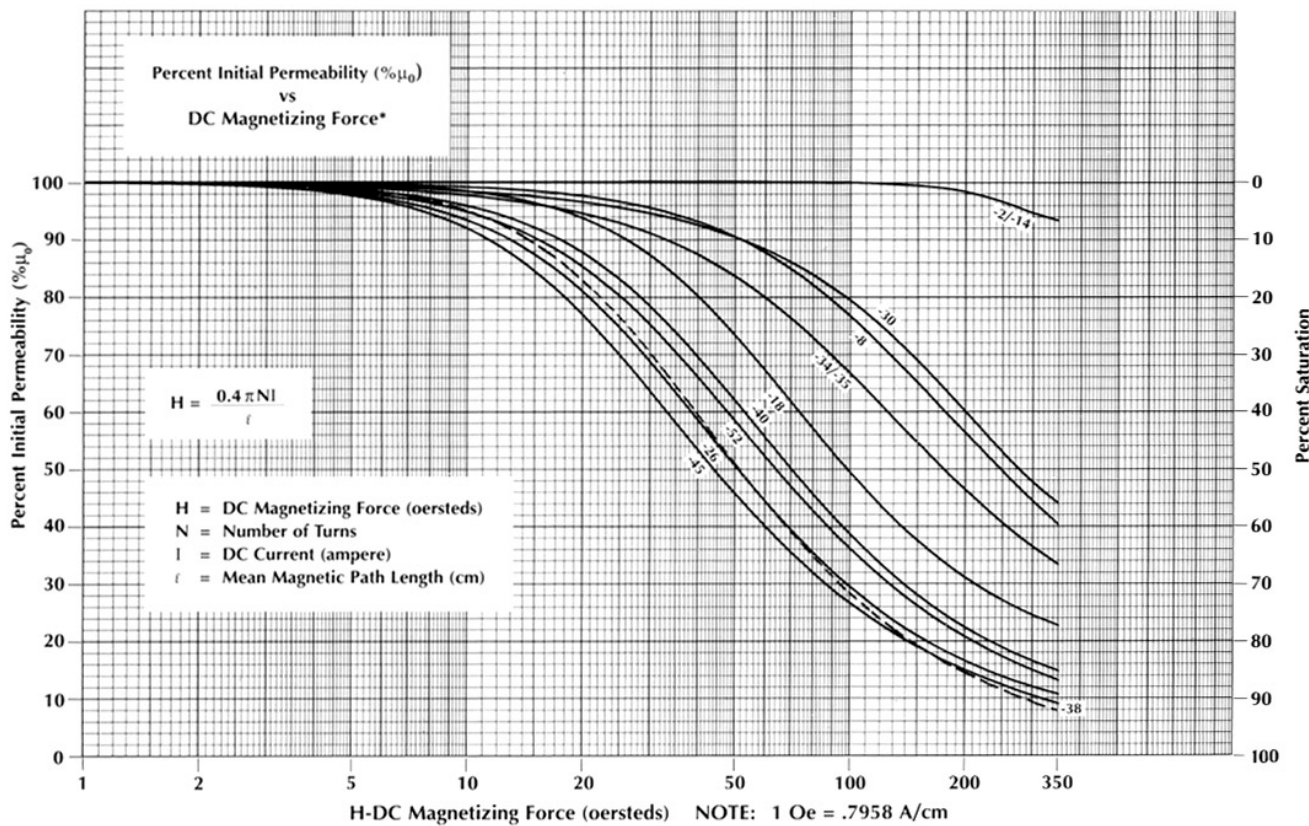
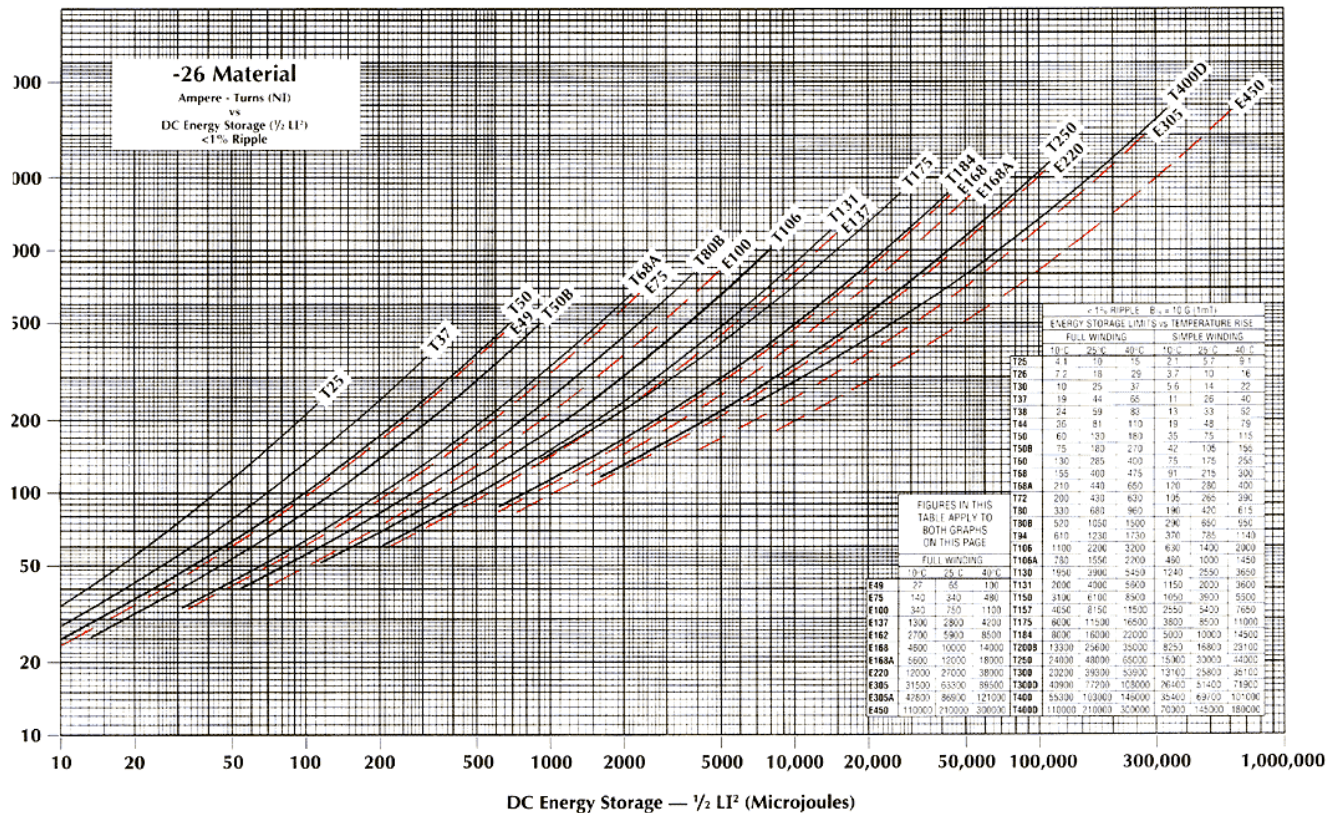


Figure B



**Figure C**

For example, the "T68" curve shows that if 150 ampere-turns are applied to this core size, that 260 microjoules of energy storage will result. Further, if 600 ampere-turns are applied, the core will store 1400  $\mu$ J of energy. These results are based the initial inductance per turn of the core and the material's saturation characteristics.

However, as earlier stated, most iron powder designs are limited by temperature rise not saturation. This graph also contains a table showing energy storage limits Vs temperature rise for two different types of windings. From this table it can be seen that if the T68 size core is wound with a "simple" winding (80% of the cores inside diameter remaining) that it can store 245  $\mu$ J for a 40  $^{\circ}$ C temperature rise. Therefore, in the above example the 150 ampere-turn, 260  $\mu$ J winding will result in slightly more than a 40  $^{\circ}$ C rise. Likewise, if a "full winding" is used (45% of the cores inside diameter remaining) the 260  $\mu$ J example will produce less than a 25  $^{\circ}$ C temperature rise. This difference in temperature rise is simply due to the wire size used.

The information in this table is based on continuous operation in freestanding air. Under these conditions, from the example above, if the T68 was wound to 600 ampere-turns in order to produce 1400  $\mu$ J, it would result in an extreme and impractical temperature rise resulting from winding losses.

**Winding Losses:** When selecting the required wire size to handle a given amount of current, "rule of thumb" formulations based on circular mills per amp are generally inadequate. The wound unit temperature rise resulting from copper losses are directly related to core size, wire size, and nature of the winding. For example, in a DC choke, with insignificant skin effect,



assuming 250 circular mils per amp for a single layer toroidal winding, #26 AWG would be selected for a 1 amp application resulting in a temperature rise of about 10 C°. Using the same "rule of thumb" for a 25 amp application, #12 AWG would be selected, this time resulting in a 40 C° temperature rise.

For single layer windings on toroidal cores, current handling capability versus temperature rise is independent of core size. Making use of this, a single layer winding table, has been developed as shown in Figure D on the following page. This table lists current ratings, in amperes, for various wire sizes for temperature rises of 10, 25, and 40 C°.

For example, the table shows that in a 3amp single-layer winding with a maximum allowable temperature rise due to copper loss of 10 C° that #19 wire should be used. If the allowable temperature rise is increased to 25 C°, the same wire can handle 5.26 amps; while a 40 C° rise will allow operation at 6.81 amps.

For "Full Windings" (45% of the toroids inside diameter remaining) a similar table has been developed as shown in Figure E on page 7. When parts are wound to a constant fill-factor, it is possible to establish ampere-turns ratings as a function of temperature rise for the different core sizes. This table lists the maximum allowable ampere-turns for 10, 25, and 40 C° temperature rise due to copper loss for both toroidal and E-cores.

Both of these tables also list the DC resistivity in milliohms per centimeter for the different wire sizes as well as the mean length per turn (MLT) for the various core sizes. This information makes it very convenient to calculate the DC resistance (in milliohms) for a given winding by simply multiplying the wire resistivity times the MLT times the number of turns.

These tables also list the "Surface Area" in cm<sup>2</sup> for the different core sizes. This number reflects the effective surface area of a typical wound component. This information is useful in determining temperature rise as a function of power dissipation. The following formula has been used to generate this information in both tables:

$$\text{Rise(C}^{\circ}\text{)} = \left[ \frac{\text{Total Power Dissipation (milliwatts)}}{\text{Surface Area (cm}^2\text{)}} \right]^{0.833}$$

While there do exist many DC output choke applications which do not have enough AC content to generate any appreciable core loss, most of the higher voltage, higher frequency DC chokes and power factor correction inductors do need to take core loss into account. Additionally, designs for 60 Hz differential-mode inductors and AC resonant inductors are quite significantly affected by core loss.



### SINGLE LAYER WINDING TABLE

WIRE SIZE (AWG)		28	26	24	22	20	19	18	17	16	15	14	13	12	11	10	TOTAL POWER DISSIPATION (WATTS) VS. TEMP. RISE			
RESISTIVITY (mΩ/cm)		2.13	1.34	.842	.530	.330	.264	.210	.166	.132	.104	.0828	.0651	.0521	.0413	.0328				
MAXIMUM AMPS 10C°		.64	.90	1.29	1.83	2.62	3.12	3.72	4.45	5.33	6.35	7.60	9.03	10.8	12.9	15.4				
PER ALLOWABLE 25C°		1.07	1.52	2.17	3.09	4.41	5.26	6.27	7.50	8.97	10.7	12.8	15.2	18.2	21.7	26.0				
TEMP. RISE 40C°		1.38	1.97	2.81	4.00	5.70	6.81	8.11	9.70	11.6	13.8	16.6	19.7	23.5	28.1	33.6				
PART No.	MLT cm/turn	SURFACE AREA (cm²)	NUMBER OF TURNS														10C°	25C°	40C°	
T16	.80	.80	9	6	4	2	1										.013	.038	.067	
T20	.96	1.16	11	8	5	3	2	1									.018	.055	.097	
T25	1.19	1.88	18	14	10	7	5	4	3	2	1						.030	.089	.157	
T26	1.74	2.67	15	11	8	5	3	2	1								.042	.127	.223	
T30	1.44	2.79	25	20	15	11	7	6	5	4	3	2	1	1			.044	.133	.233	
T37	1.53	3.77	37	29	22	17	12	11	9	7	6	5	4	3	2	1	.060	.180	.316	
T38	1.92	4.43	31	24	18	13	10	8	7	5	4	3	2	2	1		.071	.211	.371	
T44	1.84	5.23	43	34	26	20	15	13	11	9	7	6	5	4	3	2	.083	.249	.437	
T50	2.01	6.86	59	47	37	28	22	19	16	14	12	10	8	7	6	4	.109	.326	.574	
T50B	2.32	7.83	59	47	37	28	22	19	16	14	12	10	8	7	6	4	.125	.373	.659	
T50D	2.95	9.87	59	47	37	28	22	19	16	14	12	10	8	7	6	4	.157	.470	.826	
T51C	2.58	7.56	36	28	22	16	12	10	9	7	6	5	4	3	2	1	.120	.360	.633	
T60	2.48	9.84	67	53	41	32	25	21	19	16	14	12	10	8	7	6	.156	.468	.824	
T60D	3.68	14.3	67	53	41	32	25	21	19	16	14	12	10	8	7	6	.228	.681	1.20	
T68	2.47	11.2	74	59	46	36	28	24	21	18	16	14	12	10	8	7	.178	.533	.936	
T68A	2.77	12.5	74	59	46	36	28	24	21	18	16	14	12	10	8	7	.198	.594	1.04	
T68D	3.41	15.2	74	59	46	36	28	24	21	18	16	14	12	10	8	7	.241	.722	1.27	
T72	3.15	13.3	54	43	33	26	19	17	14	12	11	9	7	6	5	4	.212	.634	1.11	
T80	2.80	15.5	103	82	64	51	39	35	30	27	23	20	17	15	13	11	.246	.736	1.30	
T80B	3.44	18.7	103	82	64	51	39	35	30	27	23	20	17	15	13	11	.298	.892	1.57	
T80D	4.07	22.0	103	82	64	51	39	35	30	27	23	20	17	15	13	11	.350	1.05	1.84	
T90	3.64	22.4	115	92	72	57	44	39	34	30	26	23	20	17	15	13	.356	1.07	1.88	
T94	3.44	22.0	117	94	74	58	45	40	35	31	27	24	21	18	15	13	.350	1.05	1.85	
T106	4.49	31.0	118	95	74	59	46	40	36	31	27	24	21	18	15	13	.492	1.47	2.59	
T106A	3.86	26.8	118	95	74	59	46	40	36	31	27	24	21	18	15	13	.427	1.28	2.25	
T106B	5.19	35.5	118	95	74	59	46	40	36	31	27	24	21	18	15	13	.565	1.69	2.97	
T124	3.95	33.3	150	120	95	75	59	52	46	40	36	31	27	24	21	18	.529	1.58	2.79	
T130	4.75	42.2	165	133	105	83	65	58	51	45	40	35	31	27	23	20	.671	2.01	3.53	
T130A	3.67	33.2	165	133	105	83	65	58	51	45	40	35	31	27	23	20	.529	1.58	2.78	
T131	5.11	42.1	134	107	85	67	52	46	41	36	32	28	24	21	18	16	.669	2.00	3.52	
T132	4.95	42.2	147	118	93	74	58	51	45	40	35	31	27	23	20	18	.671	2.01	3.53	
T141	4.75	46.8	188	151	119	95	75	66	59	52	46	40	35	31	27	24	.744	2.23	3.92	
T150	5.28	53.2	180	145	114	91	71	63	56	49	44	38	34	29	26	22	.846	2.53	4.45	
T157	5.89	63.2	204	164	129	103	81	72	64	56	50	44	39	34	30	26	.101	3.01	5.29	
T175	6.58	79.1	230	186	147	117	92	82	73	64	57	50	44	39	34	30	1.26	3.76	6.16	
T184	7.54	89.2	202	163	129	102	81	72	63	56	50	44	38	34	29	26	2.27	6.79	11.9	
T200	6.50	90.9	270	217	172	137	108	96	86	76	67	60	53	46	41	36	31	1.45	4.33	7.61
T200B	8.78	120	270	217	172	137	108	96	86	76	67	60	53	46	41	36	31	1.91	5.74	10.1
T201	8.90	111	202	163	129	102	81	72	63	56	50	44	38	34	29	26	22	1.76	5.28	9.28
T225	6.93	109	305	245	195	155	123	109	97	86	76	68	60	53	46	41	36	1.74	5.21	9.16
T225B	9.21	143	305	245	195	155	123	109	97	86	76	68	60	53	46	41	36	2.27	6.79	11.9
T250	10.4	166	270	217	172	137	108	96	86	76	67	60	53	46	41	36	31	2.63	7.88	13.9
T300	7.95	173	422	341	271	216	171	153	136	121	108	96	85	75	66	58	52	2.75	8.23	14.5
T300D	10.5	223	422	341	271	216	171	153	136	121	108	96	85	75	66	58	52	3.55	10.6	18.7
T400	11.1	301	494	399	317	254	201	179	160	142	126	113	100	88	78	69	61	4.79	14.3	25.2
T400D	14.4	384	494	399	317	254	201	179	160	142	126	113	100	88	78	69	61	6.10	18.2	32.1
T520	13.7	496	680	550	437	350	278	248	221	197	176	156	139	123	109	97	86	7.88	23.6	41.5
T520D	17.7	629	680	550	437	350	278	248	221	197	176	156	139	123	109	97	86	10.0	30.0	52.7
T650	23.1	986	769	621	494	396	315	281	250	223	199	177	158	139	124	110	98	15.7	46.9	82.5

Figure D



**"FULL WINDING" TABLE (45% TOROID ID REMAINING)**

WIRE SIZE (AWG)		28	26	24	22	20	19	18	17	16	15	14	13	12	11	10	AMPERE TURNS VS. TEMP. RISE DUE TO COPPER LOSS			TOTAL POWER DISSIPATION (WATTS) VS. TEMP. RISE			
RESISTIVITY (mΩ/cm)		2.13	1.34	.842	.530	.330	.264	.210	.166	.132	.104	.0828	.0651	.0521	.0413	10C°	25C°	40C°	10C°	25C°	40C°		
PART No.	MLT cm/turn	NUMBER OF TURNS																					
T16	.80	.80	13	8	5	3	2	1	1	1							10	17	23	.013	.038	.067	
T20	.96	1.16	16	6	4	2	2	1	1	1	1						12	21	29	.018	.055	.097	
T25	1.19	1.88	30	20	12	8	5	4	3	2	2	1	1	1			19	34	45	.030	.089	.157	
T26	1.74	2.67	23	15	9	6	4	3	2	2	1	1	1				16	29	39	.042	.127	.223	
T30	1.44	2.79	48	32	20	13	8	6	5	4	3	2	2	1	1		27	47	62	.044	.133	.233	
T37	1.53	3.77	90	59	37	24	15	12	9	7	6	5	4	3	2	2	1	42	72	96	.060	.180	.316
T38	1.92	4.43	65	43	27	17	11	9	7	5	4	3	2	2	1	1		34	60	79	.071	.211	.371
T44	1.84	5.23	112	73	46	30	19	15	12	9	7	6	5	3	3	2	2	50	87	110	.083	.249	.437
T50	2.01	6.86	196	128	81	52	33	26	21	17	13	10	8	6	5	4	3	73	120	160	.109	.326	.574
T51C	2.58	7.56	85	56	35	23	14	11	9	7	6	4	3	3	2	1	1	44	77	100	.120	.360	.633
T60	2.48	9.84	241	158	100	65	41	33	26	21	16	13	10	8	6	5	4	87	150	200	.156	.468	.824
T68	2.47	11.2	293	192	122	78	50	40	32	25	20	16	13	10	8	6	5	100	170	230	.178	.533	.936
T72	3.15	13.3	168	110	69	45	28	22	18	14	11	9	7	5	4	3	3	75	130	170	.212	.634	.111
T80	2.80	15.5	525	343	218	141	89	71	57	45	36	29	23	18	14	11	9	150	260	340	.246	.736	.130
T90	3.64	22.4	648	424	269	174	110	88	70	56	45	36	28	22	18	14	11	170	300	400	.356	1.07	.88
T94	3.44	22.0	672	440	279	180	114	91	73	58	46	37	29	23	18	14	11	180	320	420	.350	1.05	.85
T106	4.49	31.0	696	455	289	187	118	95	75	60	48	38	30	24	19	15	12	190	330	440	.492	1.47	2.59
T124	3.95	33.3	1080	707	449	290	184	147	117	93	75	60	47	37	30	23	19	260	460	610	.529	1.58	2.79
T130	4.75	42.2	1303	853	542	350	222	177	142	113	90	72	57	45	36	28	23	300	520	690	.671	2.01	3.53
T131	5.11	42.1	877	574	365	236	149	119	95	76	61	48	38	30	24	19	15	240	410	550	.669	2.00	3.52
T132	4.95	42.2	1050	687	437	282	179	143	114	91	73	58	46	36	29	23	18	260	460	610	.671	2.01	3.53
T141	4.75	46.8	1659	1086	690	446	283	226	180	144	115	92	73	57	46	36	29	360	620	820	.744	2.23	3.92
T150	5.28	53.2	1530	1002	636	411	261	208	166	132	106	85	67	53	42	33	27	350	600	800	.846	2.53	4.45
T157	5.89	63.2	1933	1266	805	520	329	263	210	168	134	107	85	67	53	42	34	400	700	930	1.01	3.01	5.29
T175	6.58	79.1	2453	1606	1021	659	418	334	267	213	170	136	108	85	68	54	43	480	830	1110	1.26	3.76	6.16
T184	7.54	89.2	1933	1266	805	520	329	263	210	168	134	107	85	67	53	42	34	420	730	970	1.42	4.25	7.47
T200	6.50	90.9	3348	2192	1393	933	571	456	365	290	232	186	148	116	93	74	59	610	1050	1400	1.45	4.33	7.61
T201	8.90	111	1933	1266	805	520	329	263	210	168	134	107	85	67	53	42	34	430	750	1000	1.76	5.28	9.28
T225	6.93	109	4230	2770	1760	1137	721	577	461	367	294	235	186	147	117	93	74	720	1260	1670	1.74	5.21	9.16
T250	10.4	166	3348	2192	1393	900	571	456	365	290	232	186	148	116	93	74	59	650	1120	1490	2.63	7.88	13.9
T300	7.95	173	7981	5227	3322	2146	1361	1089	870	693	554	443	352	278	221	176	140	1170	2030	2690	2.75	8.23	14.5
T400	11.1	301	10.8K	7104	4515	2916	1850	1480	1182	942	754	602	479	378	301	240	191	1530	2650	3510	4.79	14.3	25.2
T520	13.7	496	20.3K	13.3K	8461	5465	3467	2773	2261	1765	1413	1129	898	708	564	450	358	2420	4180	5550	7.88	23.6	41.5
T650	23.1	986	26.2K	17.2K	10.9K	7057	4477	3581	2861	2280	1824	1458	1159	914	729	581	463	2980	5170	6850	15.7	46.9	82.5

**E CORES**

E49	2.54	5.09	96	48	30	21	12	10	8	4	3	3	2	2	1	0	0	41	72	96	.081	.242	.426
E75	3.81	11.2	250	160	96	60	40	24	21	18	12	10	8	4	3	3	2	74	120	170	.178	.532	.936
E100	5.08	18.1	351	242	136	98	55	45	32	28	18	15	10	8	8	6	3	100	170	220	.289	.864	1.52
E118	5.38	29.6	598	370	232	161	90	80	56	52	33	30	18	16	14	12	5	150	270	360	.470	1.41	2.48
E125	6.42	34.4	637	390	248	175	100	90	64	56	36	33	18	16	14	12	6	150	270	360	.547	1.64	2.88
E137	6.99	36.4	731	442	297	176	119	90	65	60	44	36	24	21	12	10	10	160	280	370	.579	1.73	3.05
E145	7.38	45.1	896	585	360	232	138	120	90	64	56	36	33	30	18	14	14	190	340	450	.717	2.15	3.77
E162	8.26	50.9	784	507	310	200	140	108	80	70	48	44	27	24	14	12	12	190	320	430	.809	2.42	4.26
E168	8.85	66.7	1460	944	564	370	240	189	144	126	95	64	60	39	33	30	18	270	470	620	1.06	3.18	5.58
E168A	9.35	73.1	1460	944	564	370	240	189	144	126	95	64	60	39	33	30	18	278	480	630	1.16	3.48	6.12
E187	9.50	67.4	952	585	396	232	161	120	90	80	56	48	33	30	18	14	14	210	370	500	1.07	3.21	5.64
E220	11.5	113	2024	1332	826	517	342	272	210	162	144	105	76	68	45	39	33	370	640	850	1.81	5.40	9.50
E225	11.4	97.6	1360	864	559	350	216	168	132	114	85	60	52	36	30	27	16	280	490	650	1.55	4.65	8.17
E305	15.5	208	3999	2600	1660	1072	689	564	420	342	272	210	162	144	105	76	68	610	1060	1400	3.30	9.88	17.4
E305A	16.3	226	3999	2600	1660	1072	689	564	420	342	272	210	162	144	105	76	68	620	1070	1400	3.59	10.8	18.9
E450	22.8	384	6298	4104	2580	1725	1100	833	704	546	420	341	280	225	176	133	102	850	1480	1970	6.10	18.3	32.1
E450H	21.1	328	6298	4104	2580	1725	1100	833	704	546	420	341	280	225									



**Core Losses:** Core losses are a result of an alternating magnetic field in a core material. The loss generated for a given material is a function of operating frequency and total flux swing ( $\Delta B$ ). The core losses are due to Hysteresis, eddy current and residual losses in the core material.

Iron powder has higher core loss than some other more expensive core materials, and it will sometimes become a limiting factor in applications with relatively high ripple current at very high frequency. Consequently, it is important to have a good understanding of the proper evaluation of core loss.

A core loss curve for the -26 Material is shown below in Figure F. (Curve-fit formulas are also provided to describe these characteristics.) The core loss characteristics are presented in milliwatts per cubic centimeter as a function of peak AC flux density. This information results from sinewave core loss measurements made on a Clarke-Hesse Wattmeter.

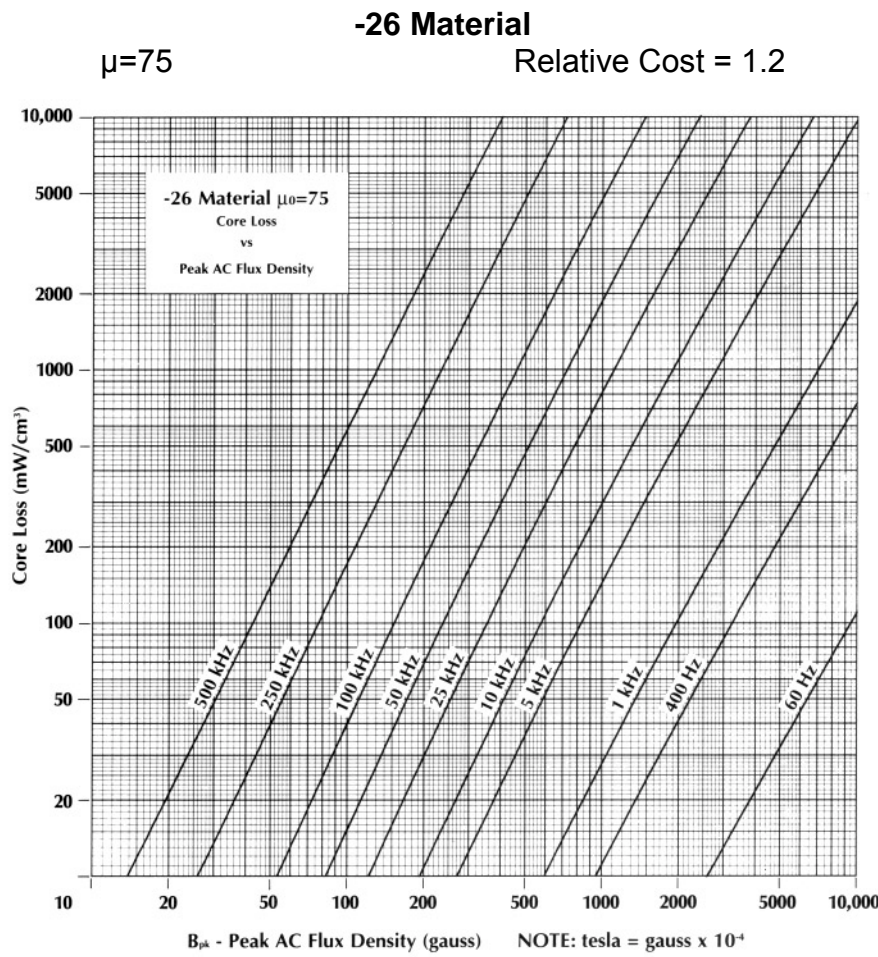


**Figure F**



A formula commonly used to calculate peak AC flux density is:

$$B_{pk} = \frac{E_{rms} \times 10^8}{4.44 \times A \times N \times f}$$

Where:

$B_{pk}$  = Peak AC flux density (gauss)

$E_{rms}$  = RMS sinewave voltage (volts)

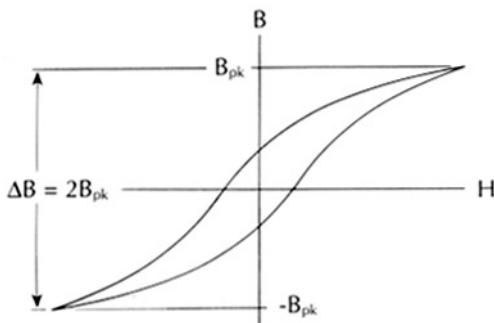
$A$  = Effective cross-sectional area ( $\text{cm}^2$ )

$N$  = Number of turns

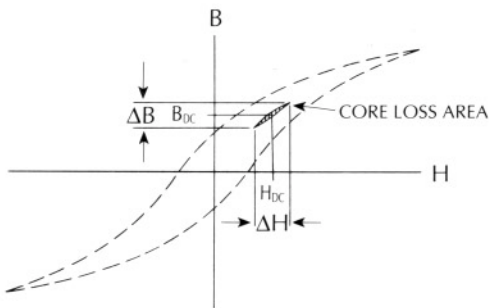
$f$  = Frequency (hertz)

This formula is useful in determining the value of peak AC flux density to be used with the core loss curves for sinewave applications such as 60 Hz differential-mode line filter inductors, resonant inductors, and for the fundamental line frequency signal in power factor correction chokes.

Under this condition, the core experiences a total peak to peak AC flux density swing ( $\Delta B$ ) that is twice the value of peak AC flux density ( $B_{pk}$ ) calculated with the preceding formula as illustrated:

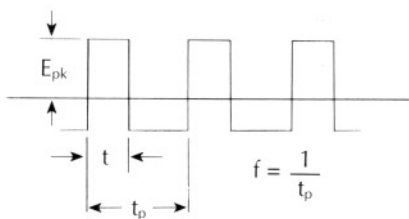


Biasing a magnetic material with DC current will shift the minor alternating BH loop but will not have a noticeable effect on the core loss. It is only the alternating flux density ( $\Delta B$ ) that generates core loss. This condition is illustrated:





The following diagram describes a typical squarewave voltage across an inductor in a switching power supply:



Since the volt-seconds ( $E_t$ ) during the "on" and "off" portion of a period must be equal in the steady-state, the peak to peak flux density for a squarewave (which is not necessarily symmetric) is described by the following formula in cgs units:

$$\Delta B = \frac{E_{pk} \times t \times 10^8}{A \times N}$$

Where:  
 $\Delta B$  = Peak to Peak flux density (gauss)  
 $E_{pk}$  = Peak voltage across coil during "t"  
 $t$  = Time of applied voltage (seconds)  
 $A$  = Cross-sectional area ( $\text{cm}^2$ )  
 $N$  = Number of turns

In unipolar applications such as flybacks, the above formulas, which describe the total peak to peak flux density, need to be used to verify operation within the maximum flux density limit of the core material in order to avoid magnetic saturation.

However, since it is industry practice to show core loss as a function of peak AC flux density with symmetrical operation about zero, the core loss curves provided assume that the peak AC flux density is half the peak to peak value ( $B_{pk} = \Delta B/2$ ). Therefore, core loss is determined from the graphs by using one-half of the peak to peak flux density at the frequency of the total period where  $f = 1/t_p$ .

The following formulas should be used to calculate the value of peak AC flux density used with the core loss graphs for most DC choke applications:

$$B_{pk} = \frac{E_{pk} \times t \times 10^8}{2 \times A \times N}$$

Where:  
 $B_{pk}$  = Peak AC flux density ( $\Delta B/2$ ) (Gauss)  
 $E_{pk}$  = Peak voltage across coil during "t" (volt)  
 $t$  = Time of applied voltage (seconds)  
 $A$  = Cross-sectional area ( $\text{cm}^2$ )  
 $N$  = Number of turns



In coupled output inductors, this same formula can be used by considering only one of the outputs; since the volt-seconds per turn are the same for all outputs and they are all working in unison.

Inductors in power factor correction boost topologies do not have the simple steady-state waveform presented previously. Rather, the high frequency signal is such that both the peak voltage across the inductor ( $E$ ) and the "on" time ( $t$ ) are constantly changing throughout the period of the fundamental line frequency (50 or 60 Hz). The core loss in this case will be the time-averaged core loss of the individual pulses for the period of the line frequency.

The flux density generated is dependent on the volt-seconds per pulse, while the core loss is dependent on approximately the square of the flux density. In order to estimate the high frequency core loss in this type of application, it is recommended that the rms value of volt-seconds during the period of the line frequency be approximated and used in the preceding formula. This will provide the value of peak AC flux density to be used with the core loss curves. The frequency is the repetition rate of the high frequency signal.

In addition to the high frequency core loss in a power factor correction inductor, the fundamental line frequency will also generate core loss. This loss should also be included when determining the total loss.

Since a cores ability to dissipate heat (surface area) varies squared with its size, but a cores generation of heat due to its magnetic losses varies cubed (volume) with its size, physically small cores can dissipate more power per unit volume than physically large cores.

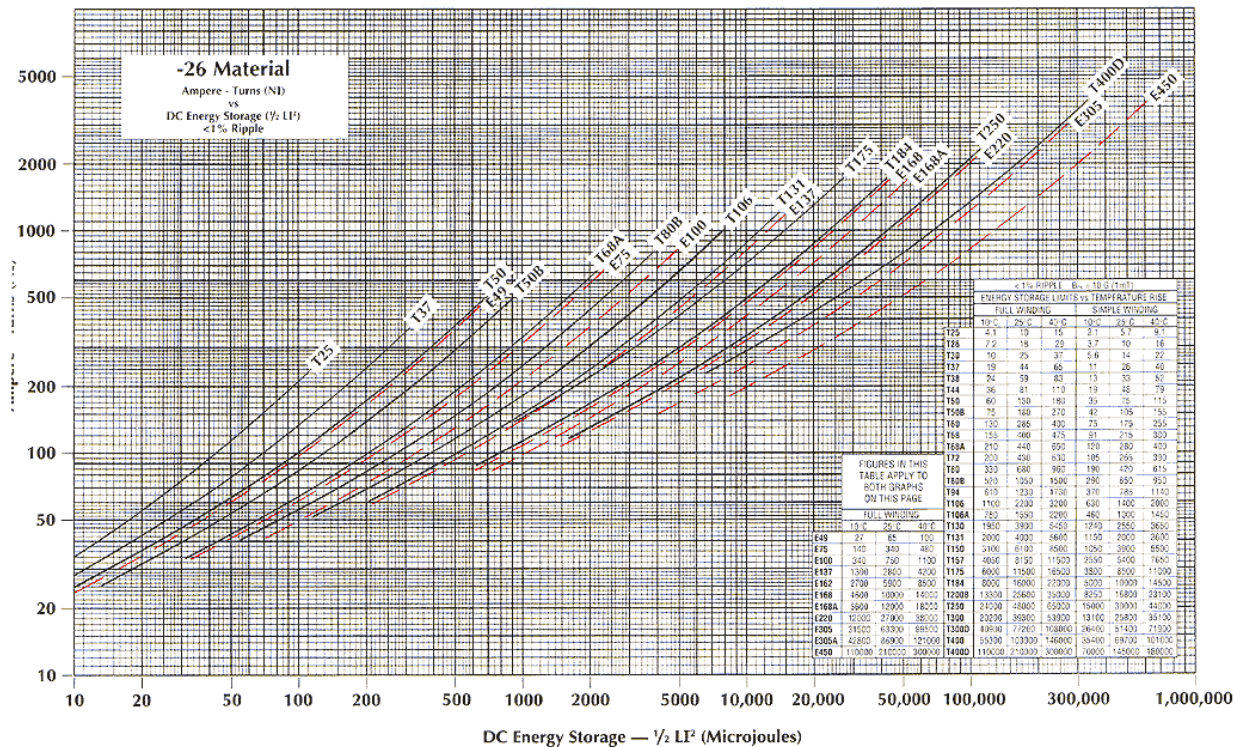
Below is a table which illustrates this through several examples: T30 is a toroidal core with an outside diameter of 0.30 inches, while T400 is a 4.00 inch outside diameter toroid.

Power Dissipation in mW/cm<sup>3</sup>  
as a function of temp. rise

Core Size	10 C°	25 C°	40 C°
T30	400	1148	2026
T50	307	874	1535
T80	212	602	1056
T94	160	454	802
T130	117	331	582
T200	87	260	436
T400	43	130	228

DC Output Inductor: Since DC flux does not generate core loss, the primary concern in most low voltage DC output inductors operating below 50 kHz becomes saturation and copper loss.

DC energy storage curves have been generated for a 1% ripple condition. The 1% ripple condition implies that this set of curves is not taking into account any effects due to AC or ripple content. These curves are based simply on DC saturation and DC winding losses. For this set of conditions, two sets of energy storage curves have been produced. These are shown on the following page, Figure G.



PART NO.	QUICK REFERENCE $A_L$ VALUES FOR -26 MATERIAL																			
	T25	T26	T30	T37	T38	T44	T50	T50B	T60	T68	T72	T80	T80B	T94	T106	T106A	T130	T131	T150	T157
A <sub>L</sub> VALUE	24.5	57.0	33.5	28.5	49.0	37.0	33.0	43.5	50.0	43.5	90.0	46.0	71.0	60.0	93.0	67.0	81.0	116	96.0	100
PART NO.	T175	T184	T200B	T250	T300	T300D	T400	T400D		E49	E75	E100	E137	E162	E168	E168A	E220	E305	E305A	E450
A <sub>L</sub> VALUE	105	169	160	242	80	160	131	262		38.0	64.0	92.0	134	210	195	232	275	287	382	540

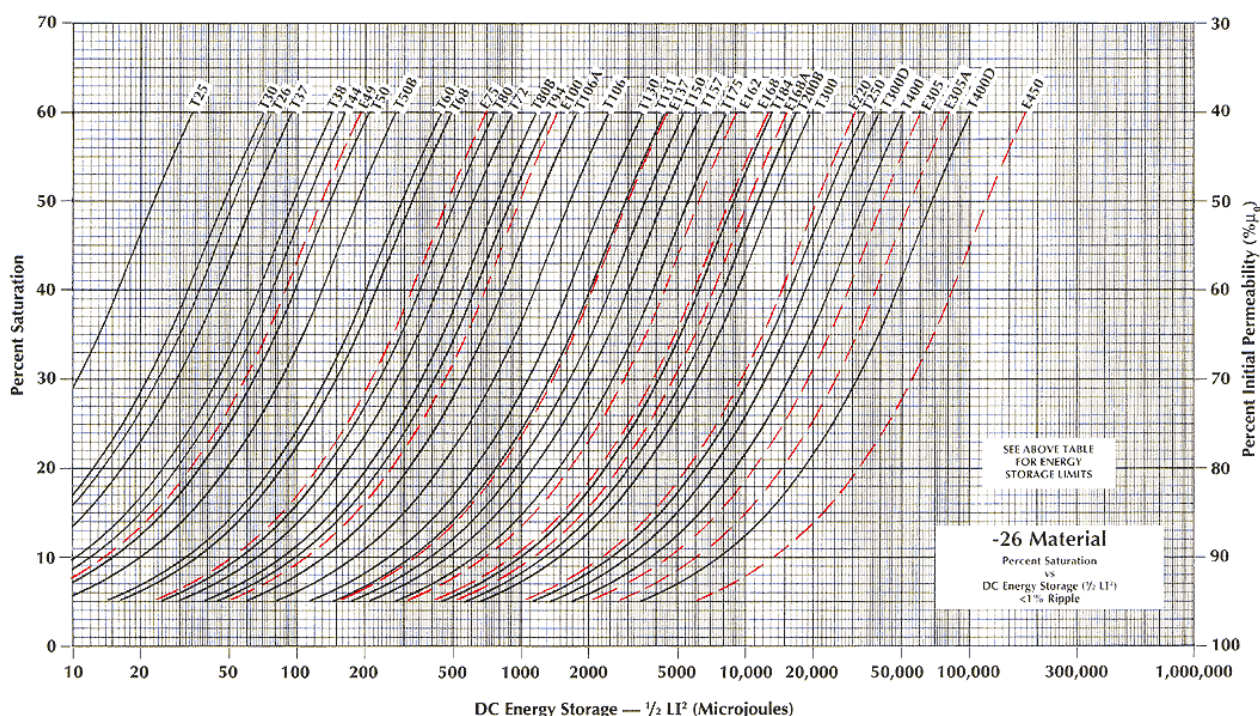


Figure G



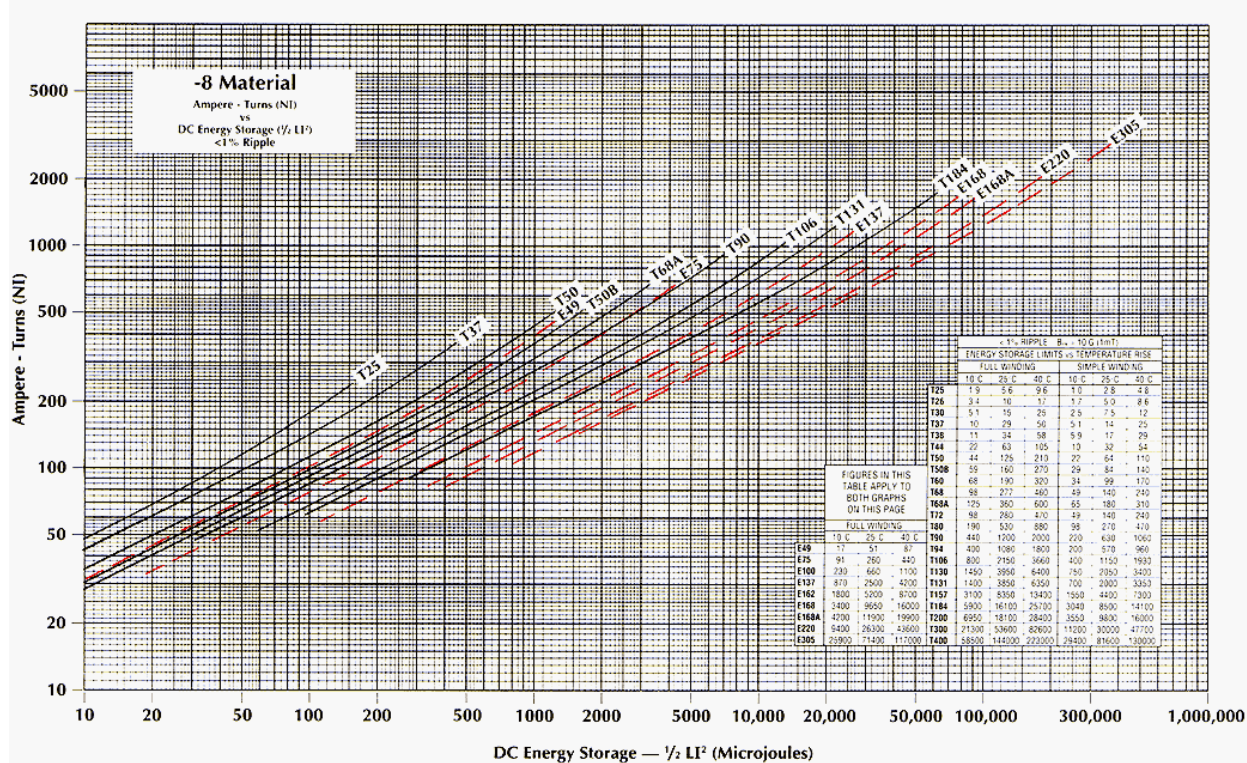
The set of curves at the top shows energy storage as a function of ampere-turns for the -26 Material. The set of curves at the bottom show energy storage as a function of percent saturation (percent saturation = 100% - percent initial permeability).

Percent saturation is a sometimes misunderstood description. What is meant by percent saturation is simply that if a core is operating at 90% of its initial permeability (90% of its low-level inductance value) then it is 10% saturated. Similarly, a core that is 30% saturated is operating at 70% of its initial permeability.

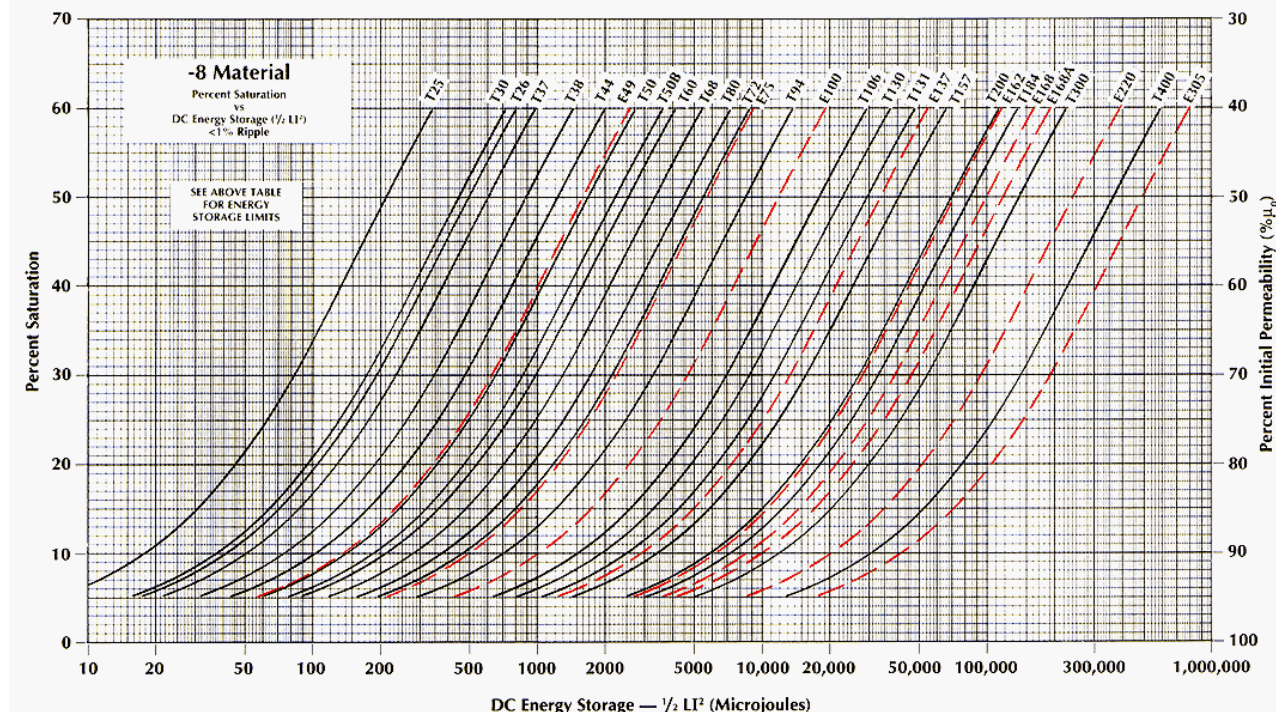
The use of both of these curves allows easy determination of required turns for a given amount of energy storage and also provides information on the amount of "swing" the inductor will have. "Swing" is a term sometimes used to describe an output chokes change in inductance with changes in operating current.

A 30  $\mu$ H, 10 amp example can be used to illustrate the use of these curves. 30  $\mu$ H, 10 amps is 1500  $\mu$ J. The table contained in the top graph shows that the T106 size core can store the required 1500  $\mu$ J with a simple winding for a 25 C° temperature rise. The curve for this core indicates that this will require about 250 ampere-turns. Since this is a 10 amp application, 25 turns will be required. Further, by referring to the graph at the bottom of the page, it can be seen that 1500  $\mu$ J will result in the core operating at 49% saturation. This means that the core will produce 59  $\mu$ H with a small amount of current flowing. By referring to the single layer-winding table it can be determined that #16 wire will fit in a single layer.

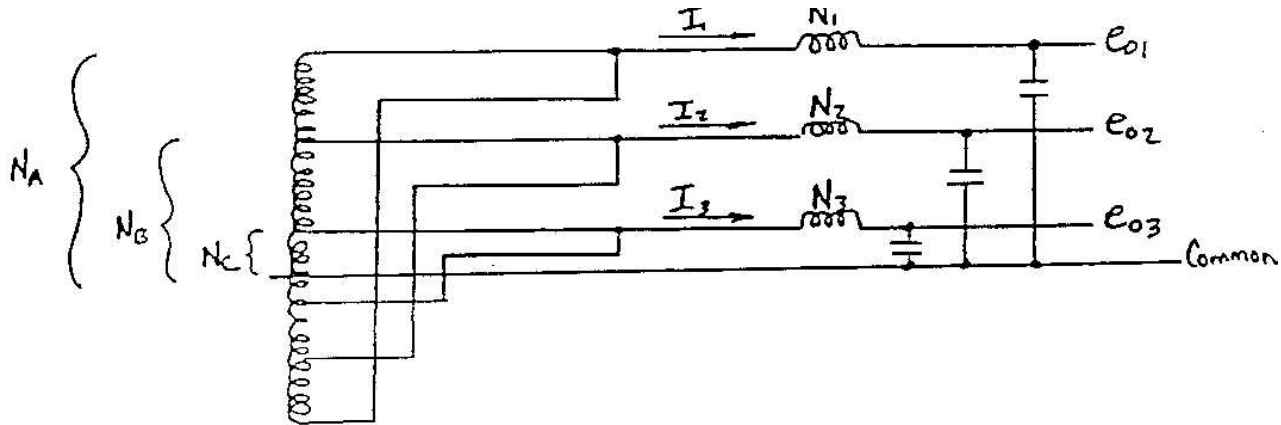
Looking at this same 30  $\mu$ H 10 amp application on the -8 Material DC energy storage curves, shown in Figure H on page 14, shows that this material can also store the required energy in the T106 size. In this case it will require 270 ampere-turns, or 27 turns of #16 wire. Referring to the curves at the bottom of the page shows that with this material, the T106 size core will be operating at only 10% saturation. This means that at low current the inductor will produce 33  $\mu$ H, which means that this material will "swing" very little.



QUICK REFERENCE $A_t$ VALUES FOR -8 MATERIAL																				
PART NO.	T25	T26	T30	T37	T38	T44	T50	T50B	T60	T68	T72	T80	T94	T106	T130	T131	T157	T184	T200	T300
$A_t$ VALUE	10.0	24.0	14.0	12.0	20.0	18.0	17.5	23.0	19.0	19.5	36.0	18.0	25.0	45.0	35.0	52.5	42.0	72.0	42.5	37.0
PART NO.	T400		E49	E75	E100	E137	E162	E168	E168A	E220	E305									
$A_t$ VALUE	60.0		20.5	33.5	48.0	67.0	105	97.0	116	143	156									


**Figure H**

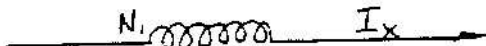
Coupled output chokes are also commonly used in multiple output supplies primarily to help improve cross regulation. The energy storage curves can still be used to assist in the design. A typical situation is illustrated below:



Proper operation of a coupled inductor requires that the turns-ratios of the transformer and coupled inductor be the same:

$$\frac{N_1}{N_A} = \frac{N_2}{N_B} = \frac{N_3}{N_C}$$

If the ampere-turns in  $N_2$  and  $N_3$  are treated as if it were all in  $N_1$ , it is possible to view the requirement as if it were a single winding choke.



$$I_x = I_1 + I_2 \frac{N_2}{N_1} + I_3 \frac{N_3}{N_1}$$

Since the ampere-turns have been treated as if they are in  $N_1$ , the required inductance for output 1 is then used with the total effective current  $I_x$  to calculate the total energy storage required:

$$\frac{1}{2} L I_x^2$$

This value of energy storage is then used to select the required E-core or toroidal core size. The energy storage curves will provide the total ampere-turns needed ( $N_1 I_x$ ) which allows easy determination for the value of  $N_1$ . The required turns-ratios determine the values of  $N_2$  and  $N_3$ .

The previous examples have assumed that the AC content of the chokes has been an insignificant consideration. While this greatly simplifies the design considerations, as operating frequencies continued to increase, the core loss consideration becomes increasingly important.

In response to the need for better core materials for high frequency output chokes, two new iron powder materials were introduced a few years ago: -18 and -52 Materials. Figure I, below, shows a brief core loss comparison of these and the other materials.

**CORE LOSS COMPARISON (mW/cm<sup>3</sup>)**
**PERMEABILITY WITH DC BIAS**

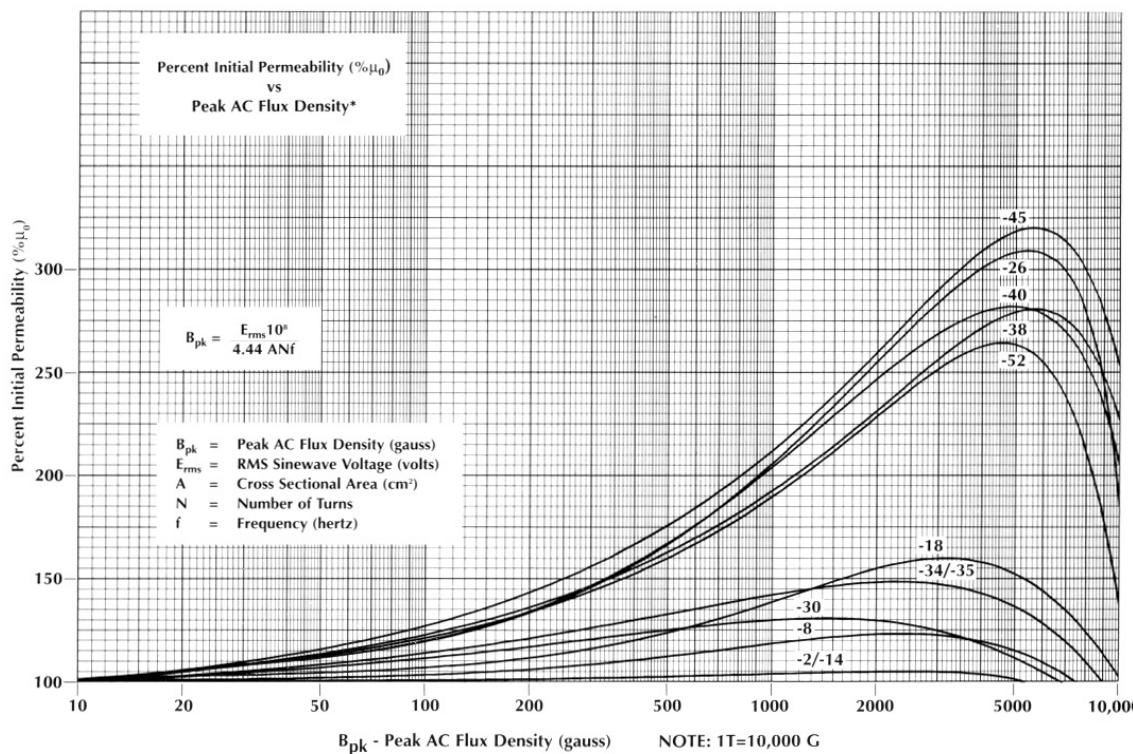
Material Mix No.	60 Hz @5000G	1kHz @1500G	10kHz @500G	50kHz @225G	100kHz @140G	500kHz @50G	HDC = 50 Oersteds % $\mu_0$	$\mu_{\text{effective}}$
-2	19 **	32 **	32 **	28	19	12	100	10.0
-8	45	64	59	50	35	28	91	31.9
-14	19 **	32 **	32 **	29	21	17	100	14.0
-18	48	72	70	63	46	37	74	40.7
-26	32	60	75	89	83	139	51	38.3
-30	37	80	120	149	129	129	91	20.0
-34	29	61	87	100	82	78	84	27.7
-35	33	73	109	137	119	123	84	27.7
-38	31	57	72	99	103	217	51	43.4
-40	29	62	93	130	127	223	62	37.2
-45	26	49	60	69	61	92	46	46.0
-52	30	56	68	72	58	63	59	44.3

\*\* Low frequency core loss is extrapolated from data measured at high frequency

**Figure I**

The -52 Material is produced to the same permeability as the -26 Material, has about 40% less core loss at frequencies above 100 kHz and is available at a similar cost. The -18 Material has higher permeability than the -8 Material, is less expensive and has similar low core loss characteristics.

In DC output chokes with elevated AC content, not only does the presence of the AC need to be considered for core loss reasons, but it will also have an effect on the inductance. A graph showing the materials response to elevated AC flux density is shown below in Figure J.


**Figure J**

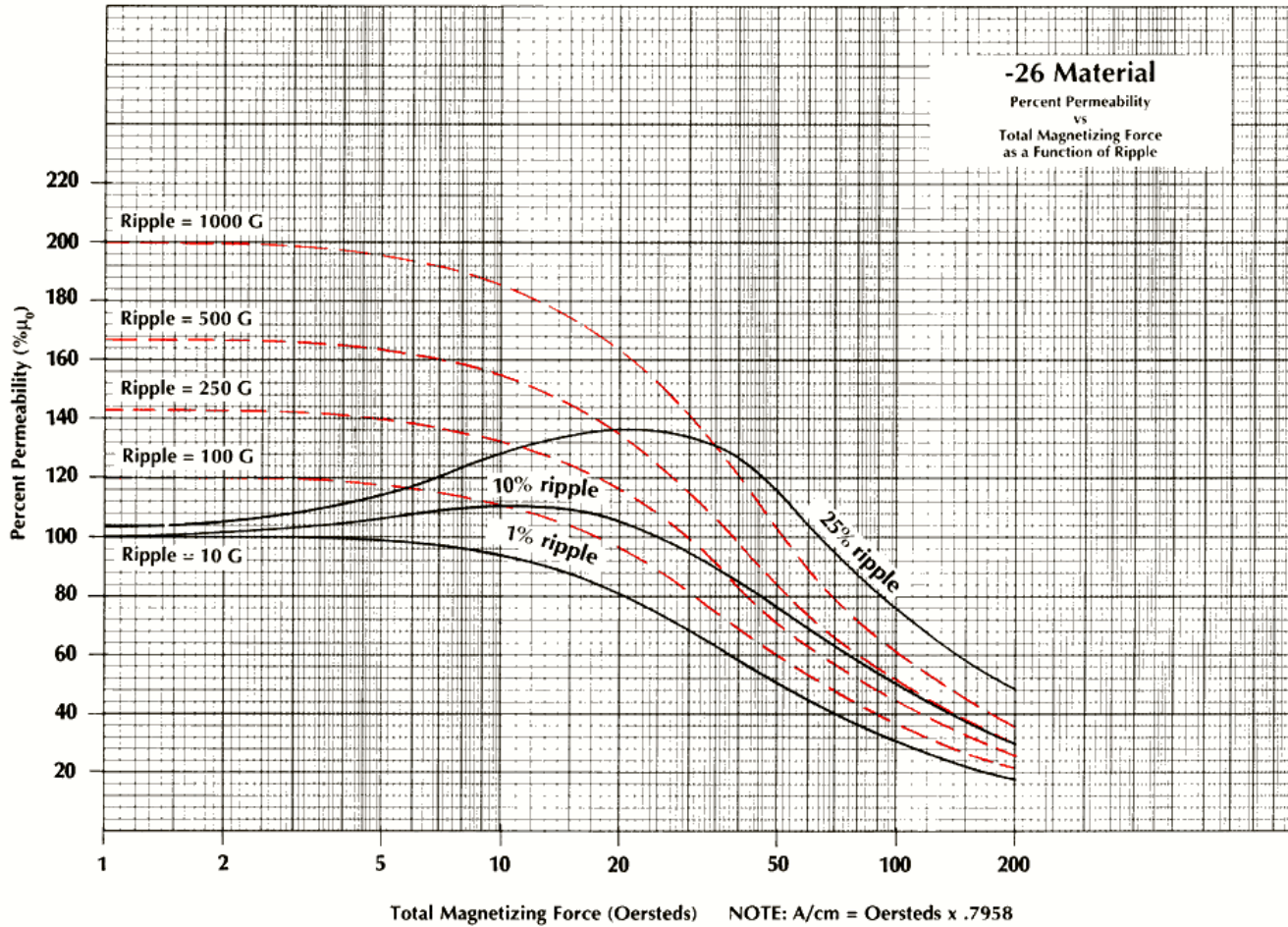


**Figure K**

When both elevated AC and DC are present a combined effect results. A graph illustrating this effect for the -26 Material is shown above in Figure K. This graph shows that while the increasing level of DC bias causes the core materials permeability to decrease, that as the level of AC increases it causes the permeability to climb. This property means that output chokes with elevated AC levels will require fewer turns than would be predicted by only considering the DC effects.

Consider the 30  $\mu$ H, 10 amp inductor described earlier. This time consider this inductor with 12.7 volts across it at 100 kHz (50% duty cycle). This inductor will be evaluated using each of the core materials on the T106 size core.

In each case, the number of turns has been determined by using the energy storage curves. This is always a good first pass approach. Since these curves do not take into account the presence of the elevated AC signal, the results with AC are somewhat different. The results shown include the effect of the elevated AC flux density.

The inductance with 12.7 volts at 100 kHz and 0 ADC is listed as well as the inductance with the 10 amps DC. This allows comparison of the relative swing of each material. The winding loss ( $I^2R$ ) and core loss resulting from the listed Bpk are also shown:

Mat'l	Turns #16	L $\mu$ H @ 0 ADC	L $\mu$ H @ 10 ADC	Bpk (G)	I <sup>2</sup> R Loss	Core Loss	Total Loss
-8	27	34.8	30.6	178	1.60	.24	1.84
-18	24	45.2	33.4	201	1.42	.34	1.76
-26	25	77.3	38.3	193	1.48	.73	2.21
-28	34	39.2	33.3	142	2.02	.75	2.77
-33	31	45.0	35.3	155	1.84	.75	2.59
-40	24	63.0	39.7	201	1.42	1.01	2.43
-52	23	68.8	42.3	209	1.36	.51	1.87

It can be seen that in all cases the inductance with DC has increased above the required 30  $\mu$ H. In most circuits this is desirable. The -18 and -8 Materials provide the lowest overall loss. These are also the most expensive core materials (relative cost 2.8 and 4.0). The -52 Material provides the next best performance and this material is considerably less expensive (relative cost 1.4).

The higher permeability material like the -26 and -52 Materials have the greatest change (about 2 times) in inductance from 0 ADC to full rated current. This swing will keep the inductor in continuous conduction to a lower current than if it did not swing. Applications requiring continuous operation down to very low loads can require a low current inductance that is 10 to 20 times that of the full current inductance.

This can be accomplished with Composite Toroids, which are made by combining a high permeability ferrite toroid with an iron powder toroid. The ferrite provides the high inductance needed under low current conditions and the iron powder provides the energy storage required under the high current conditions. The DC saturation characteristics are shown below:

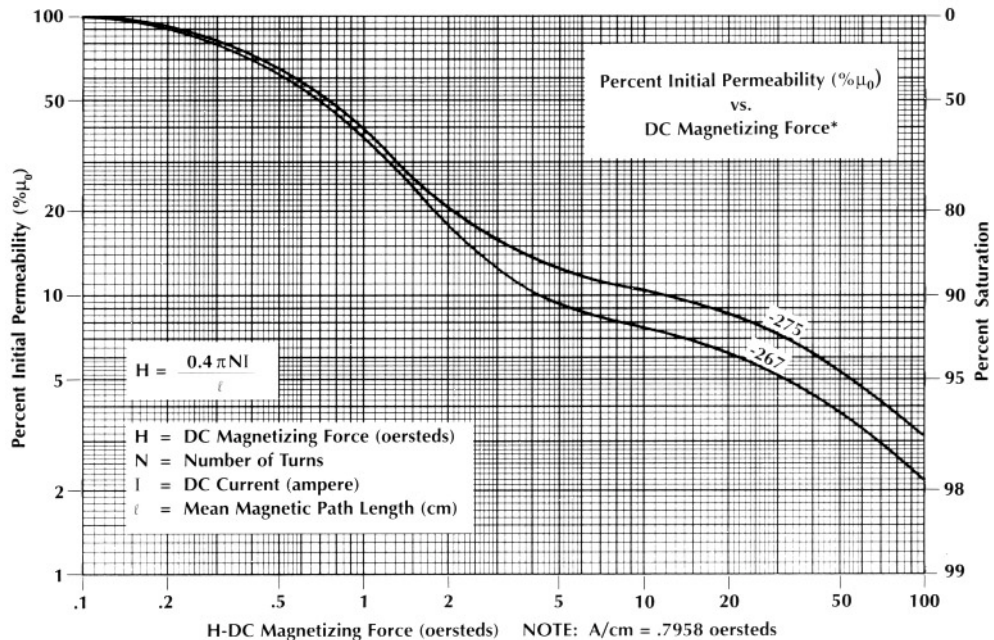


Figure L



Power factor correction inductors contain both a bias current and a lower level high frequency signal. These inductors in typical boost topologies see both a continually changing bias current (50 or 60 Hz) as well as a continually changing high frequency ripple condition. The combination of these two effects makes the evaluation of these inductors more complicated than typical DC chokes. The core loss considerations are discussed on page 11. It is generally recommended that the bias current be treated as DC current. This will provide the most conservative design.

**60 Hz Line Filter Inductors:** A typical inductor requirement in a switch-mode power supply is in the 60 Hz line filter. The high frequency to be filtered in this application falls into two categories: common-mode and differential-mode noise. Briefly, common-mode noise is noise that is common to both the hot and neutral lines in relation to earth ground. Differential-mode noise is the noise between the hot and neutral lines.

The common-mode filtering requires capacitors to earth ground. Safety regulations limit these capacitors to a relatively low value. This mandated low value of capacitance for common-mode filtering makes a high value of inductance essential to effective filtering. Common-mode inductors typically require a minimum inductance of 1000  $\mu$ H and are most often wound in a balun configuration on a high permeability core; typically a 5000 or higher permeability ferrite. The balun winding allows the 60 Hz flux generated by each line to cancel in the core, thus avoiding saturation. Lower permeability materials like iron powder can be used in this application, but the increased core size to accommodate the number of turns needed to achieve the required inductance makes this alternative less attractive.

The differential-mode inductors, however, must be able to support significant 60 Hz flux without saturating and at the same time respond to the high frequency noise. Iron powder is well suited for this requirement.

A graph of percent permeability versus peak AC flux density was shown previously in Figure J on page 16. This graph shows that the saturation flux density of the materials is greater than 10,000 gauss (it ultimately reaches about 14,000 gauss). It also shows that the higher permeability materials like the -26 Material increase in permeability quite significantly in the presence of elevated AC flux density.

Referring back to the -26 Material core loss information in Figure F on page 8, it can be seen that at a frequency of 60 Hz this material can operate at very high AC flux density without generating excessive core loss. It can also be seen that the core loss characteristics of this material are fairly high at the higher frequencies. These losses produce a coil with low Q at high frequency. This characteristic is of additional benefit in helping to suppress the unwanted signals.

60 Hz energy storage curves are provided which are based on the core materials response to AC flux density as described in Figure J. While the 60 Hz signal experiences these effects, it is not clear if the low-level noise signal experiences the same increased permeability. The most conservative design approach is to consider the 60 Hz current as DC current.

**Resonant AC Inductors:** Another use for energy storage inductors is in AC resonant applications. This type of inductor is being driven by all high frequency AC current. In order to keep the core loss to an acceptable level, it is necessary to minimize the operating flux density. This is accomplished by utilizing lower permeability materials that will require more



turns so that the same amount of voltage drop (same current flowing) will result in a lower operating AC flux density.

One method of lowering effective permeability and thus lowering the operating flux density is to introduce a localized air gap. At frequencies above 100 kHz, the additional "gap loss" generated by the high frequency fringing can cause severe localized heating problems. In many instances, the "gap loss" alone can be greater than the calculated core loss.

Iron powder has been produced for many years for use in high power communication circuits operating from 500 kHz to several MHz. One of the materials which is gaining popularity in resonant power supply applications is the -2 Material. This material has a permeability of 10 which helps keep the operating flux density low without creating localized gap-loss problems. At these high frequencies, the use on litz wire is essential in minimizing the AC winding losses.

Figure M, at the top of the following page, shows the core loss characteristics of the -2 Material up to a frequency of 2.5 MHz. This information has been used to produce Figure N at the bottom of the same page.

This graph illustrates AC RMS current as a function of inductance for the -2 Material when operated at a frequency of 1 MHz. This information is based on limiting the temperature rise resulting from core loss to 25 C°.

While the -2 Material is the material of choice for resonant applications above 20 kHz, the -30 Material should be considered for lower frequency AC inductors in very high power UPS applications operating in the 1 kHz to 5 kHz frequency range. This material provides a good balance of permeability, core loss, saturation characteristics, and core cost.

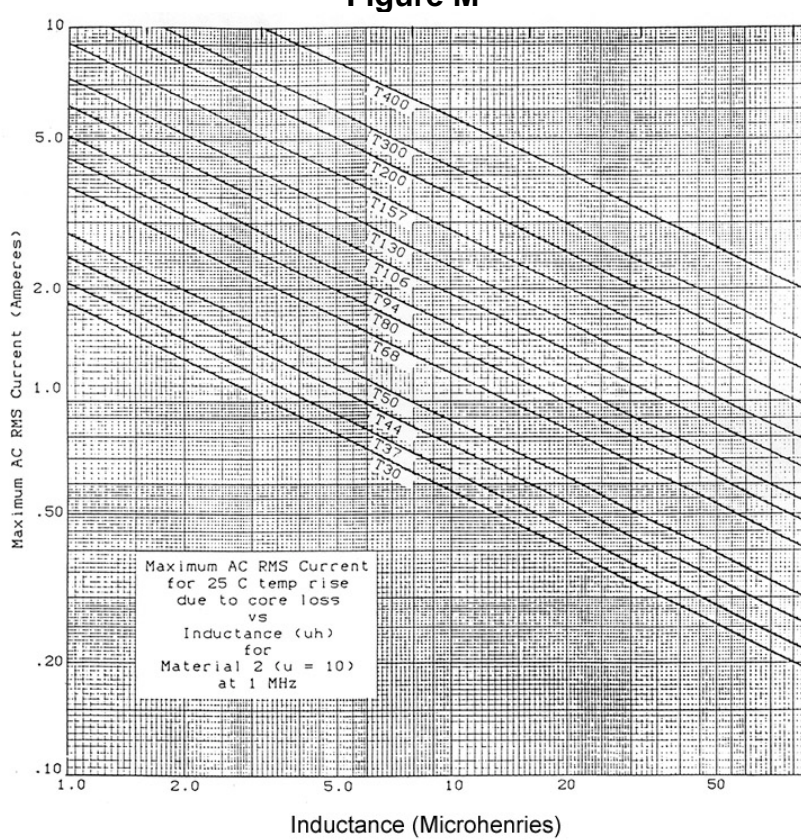
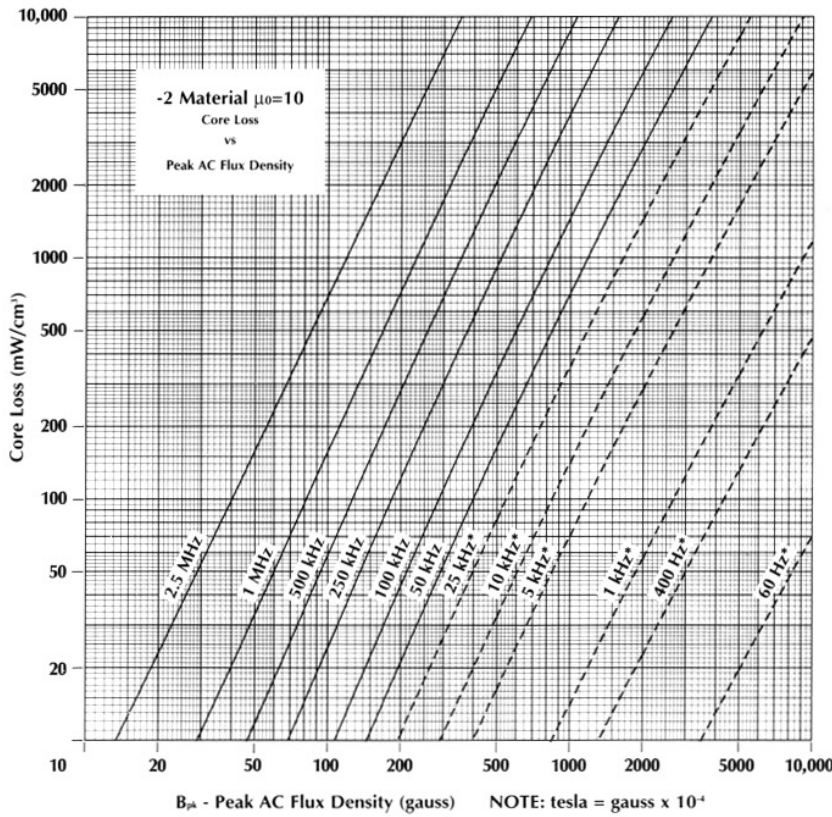


**Figure N**



**Summary:** An overview of iron powder as a core material has been presented. It has been shown that its magnetic characteristics make it well suited for a number of different inductor applications in switch-mode power supplies. It is one of the least inexpensive core materials available and is being widely used in today's commercial switching power supply industry.